CrossMark

RESEARCH PAPER

Metal Complexes of Heterocyclic Hydrazone Schiff-Bases: Preparation, Spectral Characterisation and Biological Study

Enaam I. Yousif[1] · Riyadh M. Ahmed[1] · Hasan A. Hasan[1] · Aeed S. Al-Fahdawi[2] · Mohamad J. Al-Jeboori[1]

Abstract New isatinic hydrazone Schiff-base ligands, namely furan-2-carboxylic acid (2-oxo-1,2-dihydro-indol-3-ylidene)-hydrazide (L^1), thiophene-2-carboxylic acid (2-oxo-1,2-dihydro-indol-3-ylidene)-hydrazide (L^2) and 2-(pyridine-2-yl-hydrazono)-1,2-dihydro-indol-3-one) (L^3) are reported. The ligands were prepared by the condensation of furan-2-carboxylic acid hydrazide (L^1), thiophene-2-carboxylic acid hydrazide (L^2), and 2-hydrazino pyridine (L^3) with isatine. Monomeric complexes were prepared from the reaction of the corresponding metal chloride with the ligands. The ligands and their nine new complexes of the general formulae $[M(L^n)_2]Cl_2$ [where M = Co(II), Zn(II) and Cd(II); n = L^1, L^2 and L^3] were characterised by spectroscopic methods (FTIR, UV–Vis, ^1H, ^{13}C NMR), elemental analysis, metal content, magnetic measurement and molar conductance. These studies revealed the formation of six coordinate complexes, in which the geometry about metal atom is a distorted octahedral. Biological activity of the ligands and their metal complexes against Gram-positive bacterial strain *Bacillus* (G^+) and Gram-negative bacteria *Ecoli* (G^-) are evaluated. The effects of prepared compounds depend on the type of tested bacteria. It is clear that the ligands and their metal complexes have a potential effect on the Gram-positive (G^+) and Gram-negative (G^-) strains of the tested bacteria.

Keywords Isatinic hydrazone Schiff-bases · Heterocyclic compounds · Transition metal complexes · Spectral and biological study

✉ Mohamad J. Al-Jeboori
mohamadaljeboori@yahoo.com

1 Department of Chemistry, College of Education for Pure Science (Ibn Al-Haitham), University of Baghdad, Adhamiyah, P.O. Box 4150, Baghdad, Iraq

2 Department of Chemistry, College of Science, University of Al-Anbar, Al-Ramadi, Iraq

1 Introduction

The greater importance of using isatine (1*H*-indole-2,3-dione) and its derivatives is due to their pharmaceutical applications and biological activity (Ali et al. 2011; Singh et al. 2010). Hydrazone compounds have played an important role in the development of coordination chemistry, due to their ability to form a range of stable complexes which have applications in different fields. These include their role in biological, medical and environmental sciences (Cohen 1967; Tarafder et al. 2002). Schiff-base ligands containing an azomethine group (–C=N–) are considered as an important class of compounds because of their capability to stabilize different metals in various oxidation states, and their complexes are extensively studied due to synthetic approach flexibility. Furthermore, the hydrazone Schiff-base ligands are a very important species for synthetic inorganic chemists as they are widely used to design compounds for biological modelling applications, in catalysis, and in the preparation of liquid crystals (Larson and Pecoraro 1991; Ramade et al. 1997; Hoshino 1998). Schiff-base ligands containing various donor atoms (such as N, O, S, etc.) show broad biological activities, and are of special interest because of the variety of ways in which they are bonded to the transition metal ions (Shi et al. 2009; Zhao et al. 2001). In this article, we have reported the synthesis and spectral characterisation of

Springer

new isatinic hydrazone Schiff-base compounds (L^1, L^2 and L^3) and their metal complexes with Co(II), Zn(II) and Cd(II) ions. In addition, biological experiments on both Gram-positive (G$^+$) and Gram-negative (G$^-$) strains of bacteria were also carried out.

2 Experimental

2.1 Materials

All reagents were commercially available and used without further purification. Solvents were distilled from appropriate drying agents immediately prior to use.

2.2 Physical Measurements

Melting points were obtained on a Buchi SMP-20 capillary melting point apparatus and are uncorrected. IR spectra were recorded as KBr discs using a Shimadzu 8400 S FTIR spectrophotometer in the range 4000–400 cm^{-1}. Electronic spectra of the prepared compounds were measured in the region 200–1100 nm for 10^{-3} M solutions in DMSO at 25 °C using a Shimadzu 160 spectrophotometer with 1.000 ± 0.001 cm^{-1} matched quartz cell. ^{1}H and ^{13}C NMR spectra were acquired in DMSO–d$_6$ solutions using a Jeol 400 MHz spectrometer with tetramethylsilane (TMS) as an internal standard for ^{1}H NMR. Metals were determined using a Shimadzu (A.A) 680 G atomic absorption spectrophotometer. Chloride was determined using potentiometer titration method on a (686–Titro processor–665Dosimat–Metrohm Swiss). Conductivity measurements were made with DMSO solutions using a PW 9526 digital conductivity meter and room temperature magnetic moments were measured with a magnetic susceptibility balance (Johnson Matthey Catalytic System Division).

3 Synthesis

3.1 Preparation of Ligands

The isatinic hydrazone ligands were synthesised adopting a conventional procedure published in literature (Menger et al. 1975), and as follows:

3.1.1 Preparation of L^1

A solution of isatine (1.0 g, 6.79 mmol) in methanol (5 mL) was added dropwise with stirring to a mixture of furan-2-carboxylic acid hydrazide (0.85 g, 6.79 mmol) in methanol (5 mL), and 4 drops of glacial acetic acid was added to the reaction mixture. The mixture was allowed to

reflux for 4 h, and then filtered off. The filtrate was allowed to slowly evaporate at room temperature to give the required compound as a pale yellow solid. Yield: 0.93 g (%54), m.p = 183 °C. IR data (cm^{-1}): 3410, 3199 v(N–H) of isatine and hydrazinic, 1697 v(C=O) of isatine, 1670 v(C=O) of hydrazone and 1622 v(C=N). NMR data (ppm), δ_H (400 MHz, DMSO-d$_6$): 6.78 (C$_2$–H), 6.91 (N–H) of hydrazinic, 6.96 (C$_{11}$–H), 7.06 (C$_3$–H), 7.38 (C$_{12}$–H), 7.48 (C$_{10}$–H), 7.63 (C$_{13}$–H), 7.95 (C$_1$–H) and 8.05 (H–N–C=O of isatine); δ_C (100.63 MHz, DMSO-d$_6$, ppm): 131.22 (C$_1$), 116.17 (C$_2$), 111.37 (C$_3$), 132.49 (C$_4$), 170.05 (C$_5$), 155.36 (C$_7$), 152.08 (C$_6$), 129.24 (C$_8$), 122.45 (C$_9$), 123.72 (C$_{10}$), 123.35 (C$_{11}$), 124.25 (C$_{12}$), 119.46 (C$_{13}$).

3.1.2 Preparation of L^2

The method used to prepare thiophene-2-carboxylic acid (2-oxo-1,2-dihydro-indol-3-ylidene) hydrazide (L^2) was similar to that for L^1, but with thiophene-2-carboxylic acid hydrazide (0.97 g, 6.79 mmol) in place of furan-2-carboxylic acid hydrazide. The quantities of other reagents used were adjusted accordingly. An identical work-up procedure gave the required compound as a pale brown solid. Yield: 1.26 g (% 68), m.p = 170 °C. IR data (cm^{-1}): 3398, 3184 v(N–H) of isatine and hydrazinic, 1693 v(C=O) of isatine, 1663 v(C=O) of hydrazide,1622 v(C=N). NMR data (ppm), δ_H (400 MHz, DMSO-d$_6$): 6.85 (N–H) of hydrazinic, 6.94 (C$_{11}$–H), 7.08 (C$_2$–H), 7.28 (C$_{12}$–H), 7.34 (C$_{10}$–H), 7.47 (C$_3$–H), 7.60 (C$_1$–H), 7.72 (C$_{13}$–H) and 8.02(–H–N–C=O of isatine); δ_C (100.63 MHz, DMSO-d$_6$, ppm): 129.59 (C$_1$), 124.50 (C$_2$), 132.18 (C$_3$), 148.58 (C$_4$), 166.96 (C$_5$), 151.56 (C$_6$), 161.34 (C$_7$), 133.72 (C$_8$), 116.11 (C$_9$), 125.37 (C$_{10}$), 123.09 (C$_{11}$), 128.65 (C$_{12}$), 110.61 (C$_{13}$). The mass spectrum of L^2 showed several peaks corresponding to successive fragmentations of the molecule. Peak detected at m/z 271.30 (4%) (M)$^+$ represents the molecular ion peak of the ligand. Other distinct peaks were observed in the spectrum at m/z 144.13 (5%), 75.09 (40%), assigned to the [M-(C$_5$H$_5$NOS)]$^+$ and [M–(C$_5$H$_5$NOS) + (C$_2$HN$_2$O)]$^+$ fragments, respectively.

3.1.3 Preparation of L^3

The method used to prepare 2-(pyridine-2-yl-hydrazono)-1,2-dihydro-indol-3-one) (L^3) was analogous to that for L^1, but with 2-hydrazino pyridine (0.74 g, 6.79 mmol) instead of furan-2-carboxylic acid hydrazide. The quantities of other reagents were adjusted accordingly, and an identical work-up procedure gave the required compound as a pale brown solid. Yield: 0.89 g (%55), m.p = 189 °C. IR data (cm^{-1}): 3300, 3151 v(N–H), 1689 v(C=O), 1622 v(C=N). NMR data (ppm), δ_H (400 MHz, DMSO-d$_6$): 7.78 (C$_1$–H), 6.93 (C$_2$–H), 7.28 (C$_3$–H), 7.01 (C$_4$–H), 7.44 (C$_{10}$–H), 7.05

(C_{11}–H), 7.10 (C_{-12}), 7.48 (C_{13}–H), 7.84 (N–H), 8.14 (C–N–H); δ_C (100.63 MHz, DMSO-d_6, ppm): 118.29 (C_4), 119.72 (C_2), 121.87 (C_{13}), 122.57 (C_9), 123.21 (C_{11}), 125.14 (C_{10}), 130.21 (C_{12}), 131.12 (C_3), 139.28 (C_8), 148.72 (C_1), 151.18 (C_6), 155.26 (C_7), 157.11 (C_5). The mass spectrum of L^3 ligand showed peak at m/z 238.24 (3%) (M)$^+$ related to the molecular ion peak of the ligand. Peaks detected at m/z 148.13 (5%), 79.09 (40%), were attributed to the $[M-(C_5H_2N_2)]^+$ and $[M-(C_5H_2N_2) + (C_2HN_2O)]^+$ fragments, respectively.

3.2 General Synthesis of the Complexes

A methanolic solution (10 mL) of the metal chloride salt (1 mmol) was added with stirring into methanolic solution of the isatinic hydrazone ligand (2 mmol) in methanol (15 mL). The reaction mixture was then refluxed for 2 h on a water bath until a coloured precipitate formed, which was collected by filtration, washed with cold ethanol (5 mL) and dried at room temperature. Elemental analysis data, colours, and yields for the complexes are given in Table 1.

3.3 Determination of Bacteriological Activity

Bioactivities were investigated using agar-well diffusion method (Rahman 2001). The wells were dug in the media with the help of a sterile metallic borer with centres at least 24 mm. Recommended concentration (100 μL) of the test sample 1 mg/mL in DMSO was introduced in the respective wells. The plates were incubated immediately at 37 °C for 20 h. Activity was determined by measuring the diameter of zones showing complete inhibition (mm). To clarify the role of DMSO in the biological screening, separate studies were carried out with the DMSO solutions only and they showed no activity against any bacterial strains.

4 Results and Discussion

4.1 Chemistry

The reaction of isatine with furan-2-carboxylic acid hydrazide, thiophene-2-carboxylic acid hydrazide and hydrazino pyridine in mole ratios 1:1 resulted in the formation of L^1, L^2 and L^3, respectively (see Scheme 1). The isatinic Schiff-base ligands were characterised by elemental analysis (Table 1), IR (Table 2), UV–Vis (Table 3) spectroscopy, ^{1}H–, ^{13}C-NMR and mass spectroscopy for L^2 and L^3 spectra. The di-electrolyte metal complexes were synthesised by mixing at reflux 2 mol of the ligands with 1 mol of the appropriate metal chloride. Monomeric complexes of the general formulae [M(L^n)$_2$]Cl$_2$ (where
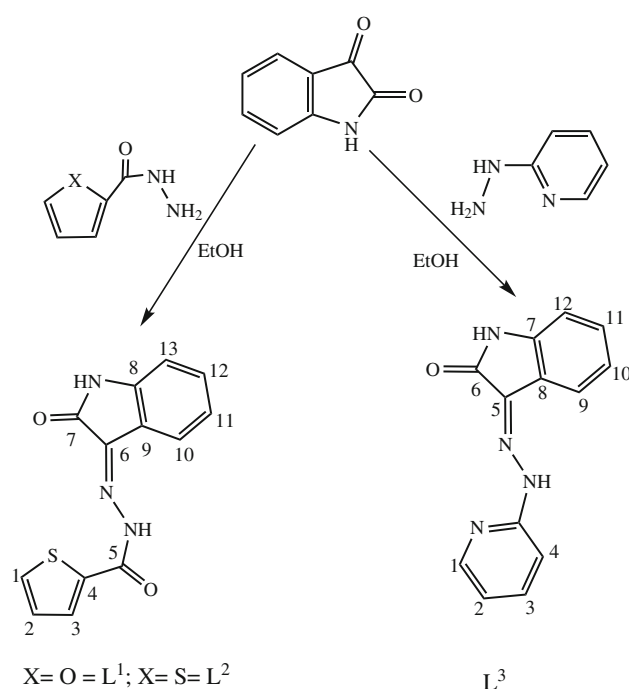
Scheme 1 Synthesis route of hydrazone Schiff-bases

$M = Co^{II}$, Zn^{II} and Cd^{II}; $n = L^1$, L^2 and L^3) were obtained (Scheme 2). The complexes are air-stable solids, soluble in DMSO and DMF. The complexes are sparingly soluble in MeOH, EtOH and not soluble in other common organic solvents. The coordination geometries of the complexes were deduced from their spectra. The analytical data (Table 1) agree well with the suggested formulae. Conductivity measurements of the complexes in DMSO solutions lie in the 68–79 cm$^2\Omega^{-1}$mol^{-1} range, indicating their 1:2 electrolytic behaviours (Geary 1971) (Table 1).

4.2 IR and NMR Spectra

The important infrared bands for the ligands and their complexes together with their assignments are listed in Table 2. The IR spectra of the ligands show characteristic bands at 1697, 1693 and 1689 cm^{-1} due to ν(C=O) of isatine moiety. Bands due to ν(C=O) of hydrazone group were observed at 1670 and 1663 in the L^1 and L^2, respectively (see supporting information(SI), Figures SI 1–3). The bands of ν(C=N) imine functional groups appeared at ca. 1622 cm^{-1}. Bands at 3410; 3199, 3398; 3184 and 3331; 3151 cm^{-1} were assigned to the ν(N–H) stretching group of isatine and hydrazinic for ligands L^1, L^2 and L^3, respectively (Al-Dulaimi et al. 2011; Al-Jeboori et al. 2005; Nakomoto 1996). The IR spectra of the complexes exhibited ligand bands with the appropriate shifts due to complex formation (Table 2). The ν(C=O) of the isatine group and ν(C=N) imine bands appeared at lower

Table l Colours, yields, elemental analyses, and molar conductance values

| Compound	Colour	Yield (%)	m.p	Found (calcd.) (%)					Λ_M (cm^2 Ω^{-1} mol^{-1})
				M	C	H	N	Cl	
L^1	Pale yellow	54	183	–	60.89 (61.18)	3.38 (3.55)	16.23 (16.46)	–	–
[Co^{II} (L^1)$_2$]Cl$_2$	Orange yellow	73	216	8.12 (9.20)	48.27 (48.77)	2.67 (2.83)	12.87 (13.13)	10.33 (11.07)	75.22
[Zn^{II} (L^1)$_2$]Cl$_2$	Yellow	54	288	9.78 (10.11)	47.58 (48.28)	2.59 (2.81)	12.33 (12.99)	9.11 (10.96)	68
[Cd^{II} (L^1)$_2$]Cl$_2$	Yellow	61	289	15.88 (16.20)	44.72 (45.01)	2.28 (2.62)	11.48 (12.11)	9.76 (10.22)	71
L^2	Brown	68	170	–	57.13 (57.55)	3.18 (3.34)	15.16 (15.49)	–	–
[Co^{II} (L^2)$_2$]Cl$_2$	Orange	73	196	7.66 (8.76)	45.82 (46.44)	2.37 (2.70)	12.19 (12.50)	9.90 (10.54)	79
[Zn^{II} (L^2)$_2$]Cl$_2$	Orange	54	270	8.54 (9.63)	45.46 (46.00)	2.24 (2.67)	11.91 (12.38)	9.01 (10.44)	71.16
[Cd^{II} (L^2)$_2$]Cl$_2$	Orange	63	274	14.93 (15.49)	41.89 (43.02)	2.24 (2.50)	10.97 (11.58)	9.26 (9.77)	77.16
L^3	Pale yellow	55	189	–	65.14 (65.54)	3.98 (4.23)	23.28 (23.52)	–	–
[Co^{II} (L^3)$_2$]Cl$_2$	Pale green	36	216	9.43 (9.72)	50.93 (51.50)	3.14 (3.32)	11.29 (18.48)	10.82 (11.69)	76.30
[Zn^{II} (L^3)$_2$]Cl$_2$	Yellow	51	273	10.24 (10.67)	50.67 (49.85)	3.11 (2.97)	17.84 (17.46)	10.83 (11.57)	74.96
[Cd^{II} (L^3)$_2$]Cl$_2$	Yellow	67	279	16.58 (17.04)	47.10 (47.33)	2.73 (3.06)	16.76 (16.98)	10.19 (10.75)	75.67

Table 2 IR frequencies (cm^{-1}) of the compounds

Compound	v(N–H) hydrazide	v(N–H) isatine	v(C=O) hydrazide	v(C=O) isatine	v(C=N)	v(C–O)	v(C–S)	v(C=N) pyrridyl	v(M–O)	v(M–N)
L^1	3410	3199	1670	1697	1622	1238	–	–		
[Co^{II} (L^1)$_2$]Cl$_2$	3388	3113	1669	1691	1610	1223	–		617	553
[Zn^{II} (L^1)$_2$]Cl$_2$	3366	3186	1670	1693	1603	1222	–	–	628	545
[Cd^{II}(L^1)$_2$]Cl$_2$	3297	3171	1671	1689	1614	1219	–	–	598	517
L^2	3398	3184	1663	1693	1622		871,1384(w)	–		
[Co^{II} (L^2)$_2$]Cl$_2$	3360	3186	1662	1684	1612		852,1378(w)	–	615	534
[Zn^{II} (L^2)$_2$]Cl$_2$	3348	3184	1662	1682	1614		840,1338(w)	–	623	563
[Cd^{II}(L^2)$_2$]Cl$_2$	3327	3147	1661	1687	1610		873, 1381(w)	–	607	519
L^3	3333	3151	–	1689	1622		–	1587		
[Co^{II} (L^3)$_2$]Cl$_2$	3319	3153	–	1685	1616		–	1596	634	561
[Zn^{II} (L^3)$_2$]Cl$_2$	3314	3155	–	1683	1613		–	1598	614	523
[Cd^{II} (L^3)$_2$]Cl$_2$	3323	3143	–	1682	1608		–	1593	626	528

frequency and were observed in the -range 1682–1693 and 1603–1616 cm^{-1}, respectively, compared with that detected in the free ligands in the range 1689–1697 and 1620–1622 cm^{-1} for the v(C=O) and v(C=N) groups, respectively. The shift of these bands to lower frequencies is due to reduced bond order in L^1, L^2 and L^3. This can be attributed to delocalisation of metal electron density (t_{2g}) to the π-system of the ligand (Al-Jeboori et al. 2009; Livingstone et al. 1975), indicating coordination oxygen of carbonyl group and nitrogen of the C=N moieties to the metal atoms (El-Sonbati et al. 2002). The v(C–O) and v(C–S) of the furan and thiophene groups which were detected at 1238 and 1384 cm^{-1} in L^1 and L^2, respectively, were shifted to lower frequencies and appeared at 1219–1223 and 1378–1381 cm^{-1} for the complexes of L^1 and L^2, respectively, indicating coordination of the oxygen and the sulphur of the rings to the metal atoms. The v(C=N) stretching of pyridine at 1587 cm^{-1} in L^3 is shifted to higher frequency and observed around 1593–1598 cm^{-1} for the complexes, indicating coordination of nitrogen of the C=N pyridine moiety to the metal atoms (Al-Jeboori et al. 2010). Further, the IR spectra of the complexes display characteristic bands for v(M–O) and v(M–N) vibration mode around 628–598, 623–607, 614–634 and 517–5553,

Table 3 U.V–Vis spectral data in DMSO solutions

Compound	μ_{eff} (BM)	Band position (λ nm)	Extinction coefficient ε_{max} ($dm^3\ mol^{-1}cm^{-1}$)	Assignments
L^1	–	251	1296	$\pi \rightarrow \pi^*$
		371	1012	$n \rightarrow \pi^*$
$[Co^{II}(L^1)_2]Cl_2$	3.91	268	1460	$\pi \rightarrow \pi^*$
		379	467	CT
		632	545	$^4T_1g^{(F)} \rightarrow {}^4A_2g^{(F)}$
$[Zn^{II}(L^1)_2]Cl_2$	Diamagnetic	267	1587	$\pi \rightarrow \pi^*$
		330	682	CT
$[Cd^{II}(L^1)_2]Cl_2$	Diamagnetic	265	1857	$\pi \rightarrow \pi^*$
L^2	–	267	1579	$\pi \rightarrow \pi^*$
		376	157	
$[Co^{II}(L^2)_2]Cl_2$	3.87	214	2898	$n \rightarrow \pi^*$
		369	259	CT
		608	303	$^4T_1g^{(F)} \rightarrow {}^4A_2g^{(F)}$
$[Zn^{II}(L^2)_2]Cl_2$	Diamagnetic	264	1547	$\pi \rightarrow \pi^*$
		362	111	CT
$[Cd^{II}(L^2)_2]Cl_2$	Diamagnetic	265	1692	$\pi \rightarrow \pi^*$
L^3	–	261	1577	$\pi \rightarrow \pi^*$
		314	2466	$n \rightarrow \pi^*$
$[Co^{II}(L^3)_2]Cl_2$	3.84	267	3743	$\pi \rightarrow \pi^*$
		375	3800	$n \rightarrow \pi^*$
		628	133	$^4T_1g^{(F)} \rightarrow {}^4A_2g^{(F)}$
$[Zn^{II}(L^3)_2]Cl_2$	Diamagnetic	270	401	$\pi \rightarrow \pi^*$
		300	779	CT
$[Cd^{II}(L^3)_2]Cl_2$	Diamagnetic	263	1768	$\pi \rightarrow \pi^*$

Scheme 2 Proposed structures of complexes
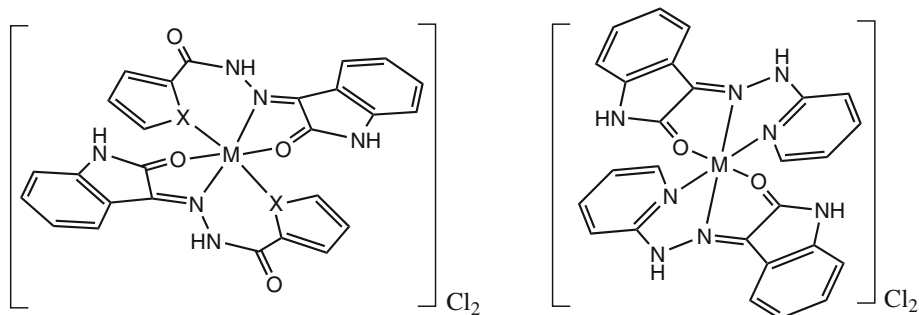
where: M= Co(II), Zn(II) or Cd(II)
X= O= L^1; X= S= L^2

where M= Co(II), Zn(II) or Cd(II)

519–563, 523–561 cm^{-1} for ligands L^1, L^2 and L^3, respectively (Al-Jeboori et al. 2009). These bands indicated that the imine nitrogen and the oxygen of the carbonyl for the ligands are involved in coordination with metal ion. The ^1H NMR spectra of the ligands in DMSO-d_6 showed peaks at 6.78–7.95, 7.8–7.60 and 6.93–7.78 ppm assigned to protons of furan, thiophene and pyridine ring for L^1, L^2

and L^3, respectively. Peaks at chemical shifts 6.91–7.84 and 8.02–8.14 ppm were assigned to N–H of hydrazinic and isatine groups, respectively (see supporting information, Figures SI 7, 9, 11). The ^{13}C NMR spectra of the ligands in DMSO-d_6 showed peaks at 152.08, 151.56 and 151.18 assigned to C_6 in L^1, L^2 and C_5 in L^3, respectively. Signals resonances at 155.36, 161.34 and 157.11 were

attributed to C_7 in L^1, L^2 and C_6 in L^3, respectively (see supporting information, Figures SI 8, 10, 12).

The ^1H NMR spectrum of the $[Zn(L^1)_2]Cl_2$ complex in DMSO-d_6 showed peaks at 7.27, 7.32 and 7.79 ppm assigned to furan ring protons. These resonances shifted downfield compared with that in free ligand, due to complex formation. The recorded peaks at 7.30, 7.52, 7.65 and 7.76 ppm were assigned to aromatic ring of isatine. The N–H of hydrazinic and isatinic groups was observed at $\delta = 8.17$ and 8.43 ppm, respectively, which are deshielded compared with that in the free ligand. This is due to coordination of carbonyl group through the lone pair electron of oxygen, and subsequently electron withdrawing from carbonyl group towards metal centre caused decrease in electron density on the N–H group (see supporting information, Figures SI 13).

4.3 Mass Spectra

The mass spectra of the ligands were also consistent with the proposed structural formulae (see "Experimental" section). The positive ion ES mass spectra for L^2 and L^3 are reported. The mass spectrum of L^2 showed several peaks corresponding to successive fragmentations of the molecule. Peak detected at m/z 271.30 (4%) (M)$^+$ represents the molecular ion peak of the ligand. Other distinct peaks were observed in the spectrum at m/z 144.13 (5%), 75.09 (40%), assigned to the $[M–(C_5H_5NOS)]^+$ and $[M–(C_5H_5\_NOS) + (C_2HN_2O)]^+$ fragments, respectively (see supporting information, Figure SI 14).

L^3 ligand showed peak at m/z 238.24 (3%) (M)$^{+1}$ related to the molecular ion peak of the ligand. Peaks detected at m/z 148.13 (5%), 79.09 (40%) were attributed to the $[M–(C_5H_2N_2)]^+$ and $[M–(C_5H_2N_2) + (C_2HN_2O)]^+$ fragments, respectively (see supporting information, Figure SI 15).

4.4 Electronic Spectra and Magnetic Measurement

The UV–Vis spectra of the ligands exhibit high intense absorption peaks around 250-267 and 314-376 nm, assigned to $\pi \rightarrow \pi^*$ and $n \rightarrow \pi^*$, respectively (Silverstein 2005) (see supporting information, Figures SI 4-6). The electronic spectra of the cobalt (II) complexes with L^1 and L^2 exhibit high intense peaks at 268 and 214, respectively, due to ligand field. While in L^3 the spectrum shows peaks at 265–300 nm related to the intra-ligand. Bands detected at 379, 369 and 375 nm were attributed to charge transfer transition for L^1, L^2 and L^3, respectively. The electronic spectra of the Co(II) complexes for L^1, L^2 and L^3 exhibited band which can be attributed to $^4T_1g^{(F)} \rightarrow ^4A_2g^{(F)}$ transition that is consistent with octahedral assignment. The magnetic moment of these complexes is typical for a high spin distorted octahedral structure (Lever 1984; Figgis 1967; Nasman 2008). The spectra of the Zn and Cd(II) complexes for L^1, L^2 and L^3

exhibited bands were assigned to $\pi \rightarrow \pi^*$ and $L \rightarrow M$ charge transfer (Lever 1984; Aly et al. 1985).

4.5 Antimicrobial Activity

The free hydrazone Schiff-base ligands and their metal complexes were screened against *Bacillus* (G$^+$) and *Ecoli* (G$^-$) to assess their potential as an antimicrobial agent by disc diffusion method, Table 4. The effects of prepared compounds depend on the type of tested bacteria. It is clear that the ligands showed different activity effect on both types of the Gram-positive (G$^+$) and Gram-negative (G$^-$) of the tested bacteria. L^1 appears to be highly active against Gram-negative (G$^-$) strain. However, L^3 is shown to be highly active against Gram-positive (G$^+$) strain. In general, complexes display a range of activity against tested strains of bacteria. $[Co^{II}(L^1)_2]Cl_2$ complex showed the highest activity against both strains, the negative Gram (G$^-$) and the positive Gram (G$^+$), among L^1-complexes. On the other hand, the Zn-complexes for L^2 and L^3 showed the highest activity against both strains of bacteria (Chohan et al. 2004).

5 Conclusion

In this paper, we have explored the synthesis and coordination chemistry of some complexes derived from the hydrazone Schiff-base ligands (L^1, L^2 and L^3). The complexes were prepared by mixing at reflux 2 mmol of the Schiff-base ligand with 1 mmol of the appropriate metal chloride. Complexes of the general formulae $[M(L^n)_2]Cl_2$

Table 4 Antibacterial activities of the synthesised Hydrazone Schiff-bases and their metal complexes

Compound	*Bacillus* (G$^+$)	*Ecoli* (G$^-$)
L^1	−	+++
$[Co^{II}(L^1)_2]Cl_2$	+++	+++
$[Zn^{II}(L^1)_2]Cl_2$	−	++
$[Cd^{II}(L^1)_2]Cl_2$	+	++
L^2	+	++
$[Co^{II}(L^2)_2]Cl_2$	−	++
$[Zn^{II}(L^2)_2]Cl_2$	+++	++
$[Cd^{II}(L^2)_2]Cl_2$	+	++
L^3	++	+
$[Co^{II}(L^3)_2]Cl_2$	−	++
$[Zn^{II}(L^3)_2]Cl_2$	++	+++
$[Cd^{II}(L^3)_2]Cl_2$	+	+

(−) = No inhibition = inactive, (+) = (2–4) mm = active, (++) = (5–7) mm = more active

(+++) = (8–13) mm = highly active

[where M=Co(II), Zn(II) and Cd(II)] were obtained. Physico-chemical analysis indicated the formation of six coordinate dicationic metal complexes. Biological activities revealed that the ligands and their metal complexes showed different activity effect on both types of the Gram-positive (G^+) and Gram-negative (G^-) of the tested bacteria.

References

Al-Dulaimi JS, Al-Jeboori MJ, Issa IO (2011) Formation of binuclear metal complexes with multidentate schiff-base oxime ligand: synthesis and spectral investigation. J Ibn Al-Haitham Pure Appl Sci 24(2):205–218

Ali MA, Mirza AH, Bakar HJ, Bernhardt PV (2011) Preparation and structural characterization of nickel(II), cobalt(II), zinc(II) and tin(IV) complexes of the isatin Schiff bases of S-methyl and S-benzyldithiocarbazates. Polyhedron 30(4):556–564

Al-Jeboori MJ, Abdul Rahman AA, Atia S (2005) Synthesis and spectral studies on cobalt(II), nickel(II), copper(II), palladium(II), platinum(II, IV), zinc(II), cadmium(II) and mercury(II) complexes of (1,2-diaminoethane-N, N-bis(2-butylidine-3one-dioxime). J Ibn Al-Haitham Pure Appl Sci 18(2):51

Al-Jeboori MJ, Al-Dujaili AH, Al-Janabi A (2009) Coordination of carbonyl oxygen in the complexes of polymeric N-crotonyl-2-hydroxyphenylazomethine. Transition Met Chem 34(1):109–113

Al-Jeboori MJ, Al-Tawel HH, Ahmad RM (2010) New metal complexes of N_2S_2 tetradentate ligands: synthesis and spectral studies. Inorg Chim Acta 363(6):1301–1305

Aly MM, Baghlaf AO, Ganji NS (1985) Linkage isomerism of the oximato group: the characterization of some mono- and binuclear square planar nickel(II) complexes of vicinal oxime-imine ligands. Polyhedron 4(7):1301–1309

Chohan ZH, Pervez H, Khan KM, Rauf A, Maharvi GM, Supuran CT (2004) Antifungal Cobalt(II), Copper(II), Nickel(II) and Zinc(II) Complexes of Furanyl-, Thiophenyl-, Pyrrolyl-, Salicylyl- and Pyridyl-derived Cephalexins. J Enzyme Inhib Med Chem 19(1):85–90

Cohen, M.D., Flavian, S., Topochemistry. Part XXIV. The luminescence properties of N-salicylideneaniline and related anils in solution. Journal of the Chemical Society B: Physical Organic, 1967: p. 317–321

El-Sonbati AZ, El-Bindary AA, Al-Sarawy AA (2002) Stereochemistry of new nitrogen containing heterocyclic aldehyde. IX. Spectroscopic studies on novel mixed-ligand complexes of Rh(III). Spectrochim Acta Part A Mol Biomol Spectrosc 58(12):2771–2778

Figgis BN (1967) Introduction to ligand fields. Wiley, New York

Geary WJ (1971) The use of conductivity measurements in organic solvents for the characterisation of coordination compounds. Coord Chem Rev 7(1):81–122

Hoshino N (1998) Liquid crystal properties of metal-salicylaldimine complexes.: chemical modifications towards lower symmetry. Coord Chem Rev 174(1):77–108

Larson EJ, Pecoraro VL (1991) The peroxide-dependent.mu.2-O bond formation of manganese complex [Mn(IV)SALPN(O)]2. J Am Chem Soc 113(10):3810–3818

Lever AB (1984) Inorganic Electronic Spectroscopy, 2nd edn. Elsevier, New York

Livingstone SE, Mayfield JH, Moore DS (1975) Thio derivatives of β-diketones and their metal chelates. XX. Magnetic moments of some ruthenium(III) chelates of fluorinated Monothio-β-diketones. Aust J Chem 28(11):2531–2533

Menger MF, Gold Smith DJ, Manden L (1975) Organic chemistry: a concise approach, 2nd edn. WA Benjamin, p 555

Nakomoto K (1996) Infrared spectra of inorganic and coordination compounds, 4th edn. Wiely, New York

Nasman OSM (2008) N_2S_2-Donor macrocycles with some transition metal ions: synthesis and characterization. J Phosphorus Sulfur Silicon Relat Elem 183(7):1541–1551

Rahman A, Choudhary M, Thomsen W (2001) Bioassay techniques for drug development. Harwood Academic, Amsterdam, The Netherlands, pp 15–18

Ramade I, Kahn O, Jeannin Y, Robert F (1997) Design and magnetic properties of a magnetically isolated GdIIICuII Pair. Crystal structures of [Gd(hfa)3Cu(salen)], [Y(hfa)3Cu(salen)], [Gd(hfa)3Cu(salen)(Meim)], and [La(hfa)3(H2O)Cu(salen)] [hfa = Hexafluoroacetylacetonato, salen = N, N'-Ethylenebis(salicylideneaminato), Meim = 1-Methylimidazole]. Inorg Chem 36(5):930–936

Shi L, Mao W, Yang Y, Zhu H (2009) Synthesis, characterization, and biological activity of a Schiff-base Zn(II) complex. J Coord Chem 62(21):3471–3477

Silverstein RM (2005) Spectrometric identification of organic compounds. 7th edn: Wiley, New York

Singh DP, Malik V, Kumar K, Sharma C, Aneja KR (2010) Macrocyclic metal complexes derived from 2,6-diaminopyridine and isatin with their antibacterial and spectroscopic studies. Spectrochim Acta Part A 76(1):45–49

Tarafder MTH, Chew K, Crouse KA, Ali AM, Yamin BM, Fun HK (2002) Synthesis and characterization of Cu(II), Ni(II) and Zn(II) metal complexes of bidentate NS isomeric Schiff bases derived from S-methyldithiocarbazate (SMDTC): bioactivity of the bidentate NS isomeric Schiff bases, some of their Cu(II), Ni(II) and Zn(II) complexes and the X-ray structure of the bis[S-methyl-β-N-(2-furyl-methyl)methylenedithiocarbazato]zinc(II) complex. Polyhedron 21(27–28):2683–2690

Zhao J, Zhao B, Liu J, Xu W, Wang Z (2001) Spectroscopy study on the photochromism of Schiff Bases N, N'-bis(salicylidene)-1,2-diaminoethane and N, N'-bis(salicylidene)-1,6-hexanediamine. Spectrochim Acta Part A Mol Biomol Spectrosc 57(1):149–154